processes

MDPI

Article

Insights on the Separation of Kraft Lignin from Betaine-Based Eutectic Solvents: A Liquid–Liquid Equilibrium and Partitioning Study

Fernanda Sossai Altoé, Dulce Maria Santos, Sérgio M. Vilas-Boas * and Mariana Conceição da Costa *

Department of Process and Product Design (DDPP), School of Chemical Engineering (FEQ), University of Campinas (UNICAMP), Av. Albert Einstein, 500, Campinas 13083-852, São Paulo, Brazil
* Correspondence: svboas@unicamp.br (S.M.V.-B.); mcdcosta@unicamp.br (M.C.d.C.)

Abstract

Lignocellulosic biomass, composed predominantly of cellulose, hemicellulose, and lignin, is the main raw material for biorefineries. Eutectic solvents (ESs) are promising green alternatives for biomass delignification due to their low cost, reduced toxicity, and high lignin solubilization capacity. However, challenges associated with lignin recovery and ES recycling hinder their industrial application. This work addresses this challenge by investigating the liquid–liquid equilibrium (LLE) and the Kraft lignin partition (K_{Lignin}) in biphasic solvent systems composed of betaine-based ES, water, and a cosolvent (1-butanol or ethyl acetate) at 298.2 K. Four hydrogen bond donors (HBDs) were used to prepare the ESs: urea, ethylene glycol, 1,3-propanediol, and 1,4-butanediol. In nearly all systems, lignin was found to preferentially partition to the top, cosolvent-rich phase, supporting the viability of this recovery approach. In general, 1-butanol created larger biphasic regions, and for the systems with 1,3-propanediol and 1,4-butanediol as HBDs, yielded higher lignin partition than ethyl acetate. The system containing 1,4-butanediol-based ES with 1-butanol was identified as the most promising, achieving exceptionally high K_{Lignin} values (up to 456.5). These results provide fundamental data for designing effective lignin recovery and ES recycling processes in biorefineries.

Keywords: Kraft lignin; eutectic mixtures; liquid–liquid equilibrium; two-phase systems; partition coefficient; sustainability; biorefinery

check for updates

Academic Editors: Zhimin Xue and Cunshan Zhou

Received: 15 October 2025
Revised: 9 November 2025
Accepted: 21 November 2025
Published: 23 November 2025

Citation: Altoé, F.S.; Santos, D.M.; Vilas-Boas, S.M.; da Costa, M.C. Insights on the Separation of Kraft Lignin from Betaine-Based Eutectic Solvents: A Liquid–Liquid Equilibrium and Partitioning Study. *Processes* **2025**, *13*, 3784. https://doi.org/10.3390/pr13123784

Copyright: © 2025 by the authors. Licensee MDPI, Basel, Switzerland. This article is an open access article distributed under the terms and conditions of the Creative Commons Attribution (CC BY) license (https://creativecommons.org/licenses/by/4.0/).

1. Introduction

The global economy remains heavily dependent on fossil fuels and petroleum-derived products to meet energy demands and supply essential chemicals, including fuel oils, polymers, and key organic compounds [1]. However, this long-term reliance is fundamentally unsustainable, as petroleum reserves are being progressively depleted due to the accelerated growth of modern society [2]. Furthermore, the combustion of fossil fuels is the primary source of anthropogenic CO_2 emissions, a major driver of the greenhouse effect and global warming [3]. To illustrate the scale of the issue, an estimated 36 billion tons of CO_2 are emitted annually to satisfy global energy and fuel demands, with fossil fuels accounting for approximately 85–90% of this total [4,5]. Consequently, there is an urgent and growing demand for more sustainable alternatives to transition away from a petroleum-based economy [2,6,7].

In this context, lignocellulosic biomass stands out as a strategic alternative, widely regarded as the only renewable resource with realistic potential to replace petroleum for both

energy generation and the production of platform chemicals [2,8]. This biomass presents low-cost, high-energy density, rich aromatic content, and widespread availability in nature [7,9]. Structurally, lignocellulosic biomass is primarily composed of two polysaccharides–cellulose (30–50%) and hemicellulose (19–45%)–and lignin (15–35%) [10]. These components are intricately interconnected, forming a recalcitrant crystalline structure that strongly resists destruction due to the presence of hydrogen bonds and Van der Waals forces, which is a primary challenge for its valorization in biorefineries [9,11].

While the polysaccharide fractions of the lignocellulosic biomass are widely valorized, lignin's potential remains far unexplored. Cellulose is used in the production of several manufactured products, including paper, food packaging films, biosorbents, cardboard, cellophane, and biofuels. Hemicellulose, on the other hand, has applications in the food and pharmaceutical industries, as well as in polymer manufacturing and chemical production, including compounds such as furfural, furfuryl alcohol, ethanol, ethyl levulinate, and γ-valerolactone [12,13].

The case of lignin, however, is quite different. As the second most abundant natural macromolecule and a rich source of aromatics, it holds significant potential in high-value products, including bioplastics, composites, resins, carbon fibers, nanoparticles, and biofuels [13–18]. Nevertheless, its chemical valorization still faces considerable challenges stemming from its complex structure, high chemical stability, and low solubility in conventional solvents [19]. As a result of these difficulties, the vast majority of lignin is underutilized [12,20]. An estimated 98% of the nearly 150 million tons of lignin generated annually by pulp and paper mills is simply burned for low-value energy recovery [6], leaving only 2% for higher value-added applications [10,12,21]. Therefore, lignin valorization becomes essential to enhance the efficiency and profitability of biorefinery processes and to ensure the full utilization of lignocellulosic biomass [22,23].

Among the most widely employed lignin extraction processes in the pulp and paper industry, the Kraft process stands out as an energy-efficient and extensively used method [24,25]. This process, however, employs harsh solvents (typically sodium hydroxide and sodium sulfide) that irreversibly alter the native lignin, resulting in a structurally complex and highly condensed material known as Kraft lignin [26–28]. This complexity hinders its characterization and limits its direct use in high-value applications [9,29,30]. However, a parallel and pressing challenge remains the valorization of the vast quantities of Kraft lignin already produced annually. Therefore, developing effective separation technologies to refine the existing industrial byproduct into more homogeneous and well-defined fractions is critical to unlocking its potential for advanced bioproducts [31–33].

In the search for greener delignification and lignin valorization technologies, eutectic solvents (ESs) have emerged as a highly promising class of solvents. They have garnered interest from the scientific community for lignocellulosic biomass pretreatment due to their evidenced ability to solubilize lignin [34–38]. Moreover, under optimized conditions, ES can achieve selective fractionation of biomass—as a result of their high lignin dissolution capacity and concomitant poor cellulose and hemicellulose dissolution capacity [39,40]—resulting in the formation of a lignin-ES-rich phase and a solid pulp composed mainly of cellulose and hemicellulose [41]. This inherent selective capacity makes ES excellent candidates for developing integrated biorefinery processes for the complete valorization of lignocellulosic biomass, given that ES are capable of selectively fractionating certain regions of lignin [41–43].

Deep eutectic solvents (DESs) are eutectic mixtures, typically composed of a hydrogen-bond acceptor (HBA) and a hydrogen-bond donor (HBD), that exhibit a significant negative deviation from the ideal thermodynamic behavior, resulting in a eutectic point temperature lower than that of the corresponding ideal liquid mixture [44–46]. Furthermore,

these systems—which generally contain at least one component that is solid at room temperature—exist as stable liquids across a certain composition range at mild operating temperatures [45]. In this work, however, the more general term "eutectic solvent" will be used to refer to the selected mixtures, as their complete solid–liquid phase diagrams are not available in the literature. In general, ES are valued for their straightforward preparation and appealing properties for a wide range of applications, including low toxicity and high biodegradability, negligible vapor pressure and low flammability, good thermal and chemical stability, and a high solubilization capacity for various compounds [45,46].

Despite the ESs' great potential in processing Kraft lignin, their industrial application is hindered by the challenge of efficient solvent recovery and recycling [9,47]. The most common strategy uses large amounts of water as an anti-solvent [48–50]. In this process, water disrupts the hydrogen-bond network of the ES, causing the solvent to dissolve in the aqueous phase while the lignin, which is sparingly soluble in water, precipitates [51]. The primary drawback of this approach, however, is the high energy costs associated with removing the large amount of water needed to recycle the ES.

To overcome the high energy costs of water-based precipitation, alternative strategies have been recently exploited, such as the use of liquid–liquid extraction processes [24,25,48,49]. This technique involves adding an organic cosolvent or a cosolvent/water mixture to the ES-lignin medium to form a biphasic system. The goal is for the lignin to be selectively partitioned into the organic phase, leaving the hydrophilic ES concentrated in the aqueous phase [48]. The viability of this approach, however, depends on the careful selection of the cosolvent and ensuring that the energy savings outweigh the costs of its recovery. Despite its promise, this strategy is a recent innovation in the context of lignin-ES recovery, and the lack of available fundamental thermodynamic data hampers its development. Key information, such as liquid–liquid equilibrium (LLE) phase diagrams and partition coefficients, is essential for process design but is largely absent in the literature. To our knowledge, only a single study from Smink and collaborators [48] has reported such data for ES-lignin systems, highlighting a knowledge gap that remains to be addressed.

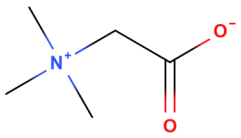
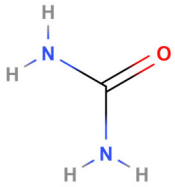
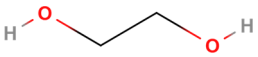
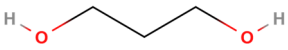
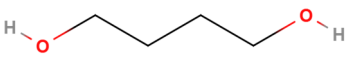
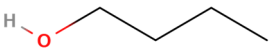
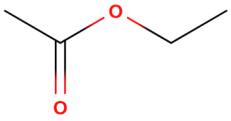
To address this knowledge gap, the present study provides new experimental LLE and lignin partitioning data in ternary systems composed of an ES, water, and an organic cosolvent at 298.15 K. For LLE studies, the binodal curves were determined using the cloud point titration method [52] and correlated with the Merchuk [53] and Hu [54] empirical models. To evaluate lignin-ES separation potential, Kraft lignin partition coefficients were also measured for the resulting biphasic systems using the shaken flask method combined with UV–vis spectroscopy [55]. The ESs investigated were prepared using betaine as HBA and for different HBDs: urea, ethylene glycol, 1,3-propanediol, and 1,4-butanediol; the cosolvents were 1-butanol and ethyl acetate. These ES precursors were selected based on their green credentials: natural origin, biodegradability, and ability to form stable molecular structures [56–59], while the cosolvents were chosen based on technical feasibility, low cost, and toxicity [60–63]. Specifically regarding betaine, unlike choline derivatives (such as choline chloride), this compound stands out for its industrial origin, being obtained from renewable sources as a by-product of sugar production, rather than from fossil sources [56,64,65]. Furthermore, betaine-based ESs have already been applied in various fields, including lignocellulosic biomass pretreatment [66,67], protein extraction [68], polyphenol extraction [57], enzymatic reactions [69], gasoline purification [70], carbon dioxide absorption [71], and electrochemical applications [72]. Despite their interesting characteristics and broad potential for application, the literature still lacks comprehensive data and in-depth studies on betaine-based ESs.

2. Materials and Methods

2.1. Materials

Eucalyptus urograndis Kraft lignin, obtained from industrial black liquor, was kindly supplied by Suzano S.A. (Suzano, Brazil). All other reactants were used as received from the supplier, without further purification. Detailed information on each compound, including chemical structure, purity, and supplier, is provided in Table 1. Bidistilled water was used throughout the experiments.

Table 1. Chemical structures, purity, and suppliers of the compounds used in this work.

Compound	Chemical Structure	Purity (%)	Supplier (CAS)
betaine (BET)		98.0	INLAB (107-43-7)
urea (U)		98.0	GIBCO BRL (57-13-6)
ethylene glycol (EG)		99.5	Dinâmica (107-21-1)
1,3-propanediol (PROP)		98.0	Sigma Aldrich (504-63-2)
1,4-butanediol (BUT)		99.0	Dinâmica (110-63-4)
1-butanol (1-But)		99.8	Sigma Aldrich (71-36-3)
ethyl acetate (EA)		99.5	ACS Científica (141-78-6)

2.2. Eutectic Solvent Preparation

The ESs were prepared using the heating and stirring method proposed by Abbott et al. [73]. In brief, betaine (BET) as the HBA was mixed with HBD–urea (U), ethylene glycol (EG), 1,3-propanediol (PROP), or 1,4-butanediol (BUT)–at a specific molar ratio. The mixture was placed in sealed glass flasks and stirred at a controlled temperature between 333.15 and 353.15 K until a clear, homogeneous liquid was formed, a process that typically required 30 to 120 min. Following preparation, the ESs were cooled to room temperature, and their final water content was determined by Karl Fischer titration (831 KF coulometer, Metrohm, Herisau, Switzerland). The specific HBA:HBD molar ratios and the measured water content for each ES are detailed in Table 2.

The molar ratios were selected based on the following rationale: the 2:3 ratio for the BET:U ES corresponds to the eutectic point reported in the literature [74] for a mixture with 2% of water; for the BET:BUT ES, the 1:9 ratio was the only composition from a wide screening (from 1:9 to 4:1) that remained a stable liquid after 12 h; and for BET:EG (1:3) and BET:PROP (1:4), the selected compositions were the lowest HBD molar ratios found to form a stable homogeneous liquid after 12 h in preliminary tests.

Table 2. Molar ratio between the HBA and HBD and water content (wt%) of the ESs prepared in this work.

HBA	HBD	Molar Ratio (HBA:HBD)	Water Content (wt%)
betaine	urea	2:3	8.14
	ethylene glycol	1:3	1.50
	1,3-propanediol	1:4	1.70
	1,4-butanediol	1:9	0.53

It is important to note that the water content values reported in Table 2 correspond to the moisture measured immediately after the preparation of the ESs, as no water was intentionally added during the process. Notably, the urea-based ESs exhibited higher water content, which is attributed to the hygroscopic nature of urea, causing it to absorb moisture from the ambient [75,76]. The ES water content was always taken into consideration in the composition calculations for all subsequent LLE and partitioning experiments.

2.3. Binodal Curve

The binodal curves of ternary systems {organic cosolvent + water + ES} were determined using the cloud-point titration method [52,55] at 298.2 K ± 0.5 K and local ambient pressure (95.0 ± 2 kPa). The procedure was carried out in a jacketed glass cell (21 cm^3) connected to a thermostatic circulating bath (TE–184, Tecnal, Piracicaba, Brazil) and placed on a magnetic stirrer (Fisatom 752, Fisatom, São Paulo, Brazil). In total, eight biphasic systems investigated resulted from the combination of the four selected ESs (BET:U, BET:EG, BET:PROP, and BET:BUT) with one of the two organic solvents, 1-butanol (1-But) or ethyl acetate (EA), in water.

To begin the titration, a known mass of water was placed in the cell under constant magnetic stirring (200 rpm). The organic cosolvent was then added dropwise until the solution became visually turbid (cloud point), indicating the formation of a second phase. Subsequently, a known amount of the ES was titrated into the biphasic system until the turbidity disappeared, restoring a single homogeneous phase. The mass of each component was recorded at the point of phase transition to determine a single point of the binodal curve. This procedure was repeated multiple times to map the entire curve and is schematically illustrated in Figure 1:

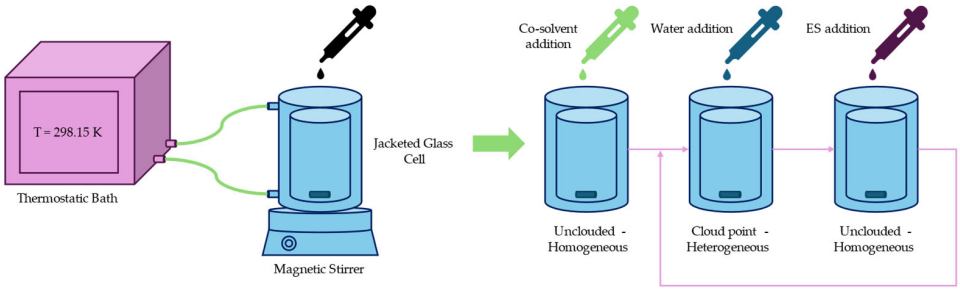


Figure 1. Process flowchart for binodal curves determination.

The mass of each component (water, cosolvent, and ES) added to the system was recorded using an analytical balance (AUY220, reproducibility of $\pm 1 \times 10^{-4}$ g, Shimadzu, Kyoto, Japan). The resulting experimental data were correlated using the empirical equation proposed by Merchuk et al. [53] (Equation (1)) and Hu et al. [54] (Equation (2)):

$$Y = Ae^{(BX^{0.5} - CX^3)} \quad (1)$$

$$Y = e^{(A+BX^{0.5}+CX+DX^2+EX^3)} \quad (2)$$

in these equations, Y and X represent the mass fractions of the cosolvent and water, respectively. The parameters *A*, *B*, *C*, *D*, and *E* are adjustable parameters obtained by non-linear regression of the experimental data. For the modeling, the ES was treated as a single pseudo-component. This pseudo-ternary approach is a necessary simplification for applying these models, which are based on a component mass balance [77–80].

The agreement between the model and experimental data was evaluated using the coefficient of determination (R^2) and the mean squared error (MSE), shown in Equation (3) and Equation (4), respectively:

$$R^2 = 1 - \frac{\sum_0^N (Y_e - Y_p)^2}{\sum_0^N (Y_e - \overline{Y}_e)^2} \quad (3)$$

$$MSE = \frac{\sum_0^N (Y_e - Y_p)^2}{N} \quad (4)$$

where Y_e and Y_p represent the experimental and predicted mass fractions of the cosolvent, respectively, $\overline{Y}_e$ is the mean of experimental mass fractions of the cosolvent, and N is the number of data points.

2.4. Kraft Lignin Partitioning

The Kraft Lignin partition coefficient (K_{Lignin}) determined in this work is defined as the ratio of lignin concentration in the top phase ($[\text{lignin}]_T$) to that in the bottom phase ($[\text{lignin}]_B$), both expressed in g·cm^3, as shown in Equation (5):

$$K_{Lignin} = \frac{[\,lignin\,]_T}{[\,lignin\,]_B} \quad (5)$$

For each system, K_{Lignin} values were determined at five distinct compositions, which were selected to fall within the biphasic region of the previously determined binodal curves. The procedure began by preparing a stock solution of Kraft lignin (~10 mg) dissolved in a known mass of corresponding ES. A sample of this stock solution was then transferred to a 15 mL centrifuge tube, along with gravimetrically known amounts of water and the organic cosolvent (AUY220, reproducibility of $\pm 1 \times 10^{-4}$ g, Shimadzu, Kyoto, Japan). The sealed tubes were homogenized by vortex (AP59, Phoenix Luferco, Araraquara, Brazil) and then placed in a thermostatic bath (MA-184, Marconi, Piracicaba, Brazil) at 298.15 ± 0.5 K for 24 h to ensure thermodynamic equilibrium was reached. After the equilibration period, the top and bottom phases were carefully separated using plastic syringes and weighed. This procedure is illustrated in Figure 2:

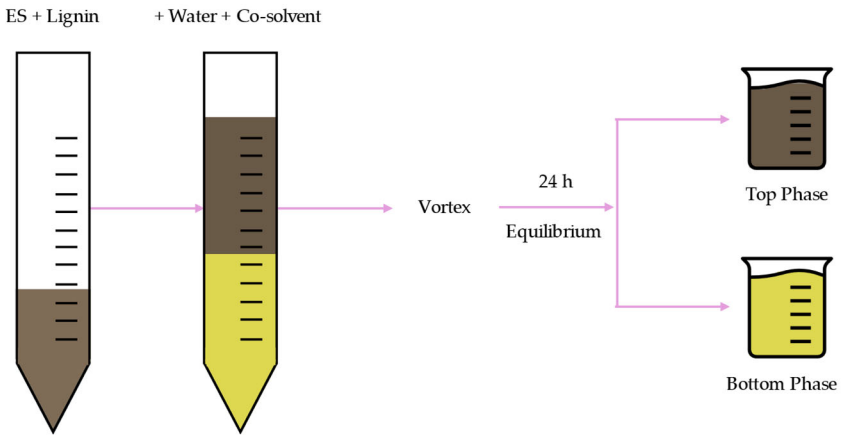


Figure 2. Process flowchart for the lignin partitioning experiments.

The density of each phase was measured using a vibrating-tube densimeter (DM45, $\pm 1 \times 10^{-5}$ g·cm^{-3}, Mettler Toledo, Columbus, OH, USA). To quantify the lignin content, a precisely weighted sample of each phase was diluted in dimethyl sulfoxide (DMSO) and its absorbance was measured at 280 nm using an UV–Vis spectrophotometer (UV-1700, Shimadzu, Kyoto, Japan). This wavelength was chosen as it is characteristic of lignin [55,81–83]. The lignin concentration in each phase was then calculated from a pre-established calibration curve (Figure S1 of the Supplementary Materials, SM), allowing for the determination of K_{Lignin} through Equation (5).

3. Results and Discussion

3.1. Phase Diagrams

The determination of LLE phase diagrams is crucial for assessing the viability of separation processes, such as fractionation and partition of biomolecules like lignin. These diagrams provide a fundamental understanding of the system's behavior at specific compositions. In this study, the ability of 1-butanol and ethyl acetate to form biphasic systems with aqueous solutions of betaine-based ESs was investigated by determining their binodal curves at 298.15 K and ambient pressure (95.0 kPa). The experimental data, reported as mass fraction (Tables S1–S8 of the SM), were correlated with the Merchuk (Equation (1)) and Hu (Equation (2)) models using the *curve_fit* function from the Python (version 3.12.11) scipy.optimize library. This function relies on the Levenberg–Marquardt algorithm [84] to perform the non-linear parameter fitting. The resulting ternary diagrams, plotted on mass fraction basis, are presented in Figures 3–6, and the adjusted parameters for Merchuk and Hu correlations are listed in Tables 3 and 4, respectively.

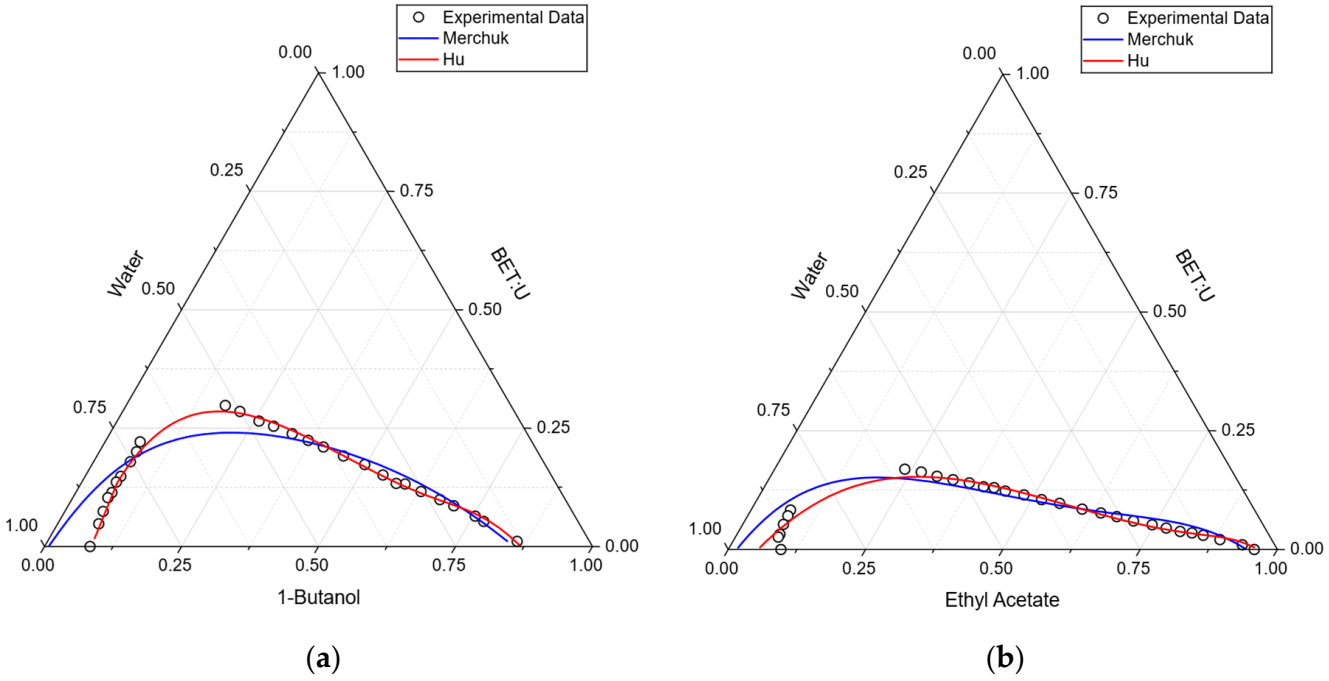


Figure 3. Ternary phase diagram of (**a**) {1-butanol + water + BET:U} and (**b**) {ethyl acetate + water + BET:U} systems at 298.15 K and 95.0 kPa. Experimental data (black circles) are compared with the correlations obtained using Merchuk (blue lines) and Hu (red lines) equations.

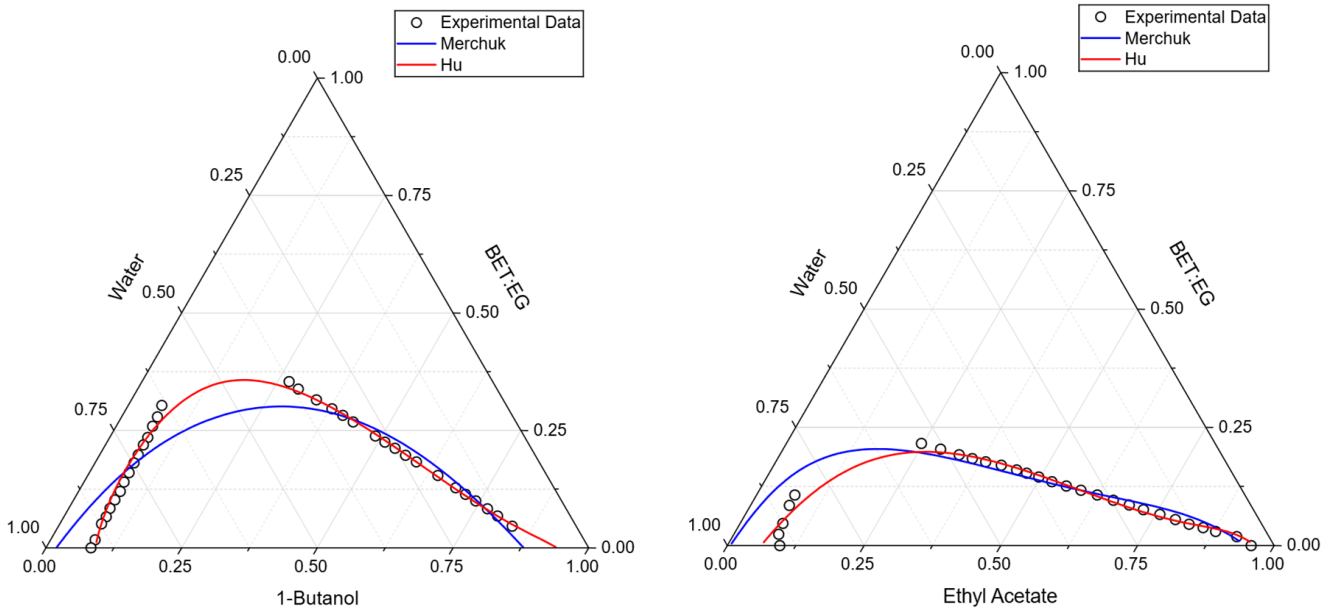


Figure 4. Ternary phase diagram of (**a**) {1-butanol + water + BET:EG} (**b**) and {ethyl acetate + water + BET:EG} systems at 298.15 K and 95.0 kPa. Experimental data (black circles) are compared with the correlations obtained using Merchuk (blue lines) and Hu (red lines) equations.

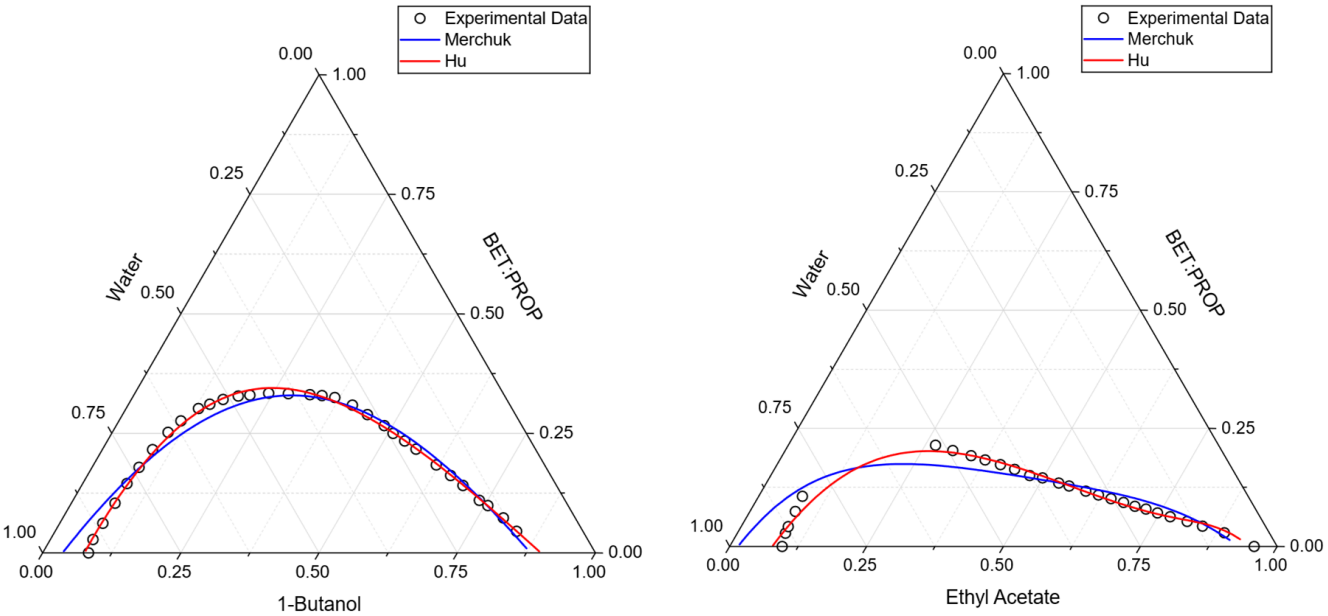


Figure 5. Ternary phase diagram of (**a**) {1-butanol + water + BET:PROP} and (**b**) {ethyl acetate + water + BET:PROP} systems at 298.15 K and 95.0 kPa. Experimental data (black circles) are compared with the correlations obtained using Merchuk (blue lines) and Hu (red lines) equations.

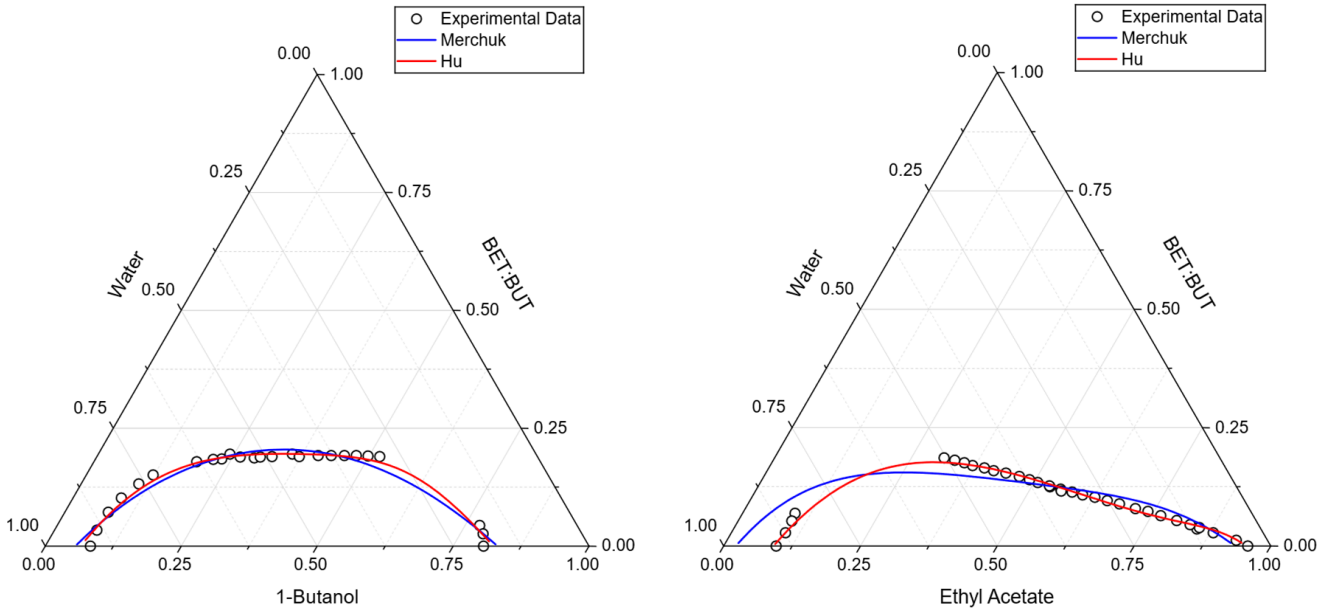


Figure 6. Ternary phase diagram of (**a**) {1-butanol + water + BET:BUT} and (**b**) {ethyl acetate + water + BET:BUT} systems at 298.15 K and 95.0 kPa. Experimental data (black circles) are compared with the correlations obtained using Merchuk (blue lines) and Hu (red lines) equations.

Table 3. Adjusted parameters and statistical metrics for the correlation of the experimental LLE data using the Merchuk equation (Equation (1)).

Cosolvent	ES	*A*	*B*	*C*	R^2	10^4 *MSE*
1-butanol	BET:U	2.129	−2.376	3.338	0.988	8.37
	BET:EG	2.845	−3.382	1.756	0.987	9.71
	BET:PROP	3.376	−3.908	0.784	0.995	3.26
	BET:BUT	2.815	−2.958	1.251	0.994	2.75
ethyl acetate	BET:U	1.216	−1.067	3.469	0.995	4.38
	BET:EG	1.236	−1.162	4.346	0.991	7.01
	BET:PROP	1.354	−1.413	3.230	0.989	7.39
	BET:BUT	1.327	−1.367	2.926	0.990	6.07

Table 4. Adjusted parameters and statistical metrics for the correlation of the experimental LLE data using the Hu equation (Equation (2)).

Cosolvent	ES	*A*	*B*	*C*	*D*	*E*	R^2	10^5 *MSE*
1-butanol	BET:U	4.922	−29.923	51.250	−59.326	31.417	0.999	4.16
	BET:EG	0.364	−3.019	6.423	−21.322	15.831	0.999	6.01
	BET:PROP	−0.043	1.765	−6.172	−0.973	2.915	1.000	3.15
	BET:BUT	7.291	−35.258	47.387	−35.650	13.371	0.995	0.21
ethyl acetate	BET:U	0.156	−1.314	1.748	−5.340	1.573	0.999	5.58
	BET:EG	0.215	−1.880	3.133	−8.726	4.310	0.999	6.11
	BET:PROP	0.486	−3.754	6.675	−12.929	6.891	0.999	5.45
	BET:BUT	0.291	−2.286	3.663	−8.835	4.609	0.999	4.26

A comparison of the phase diagrams reveals a clear trend based on the hydrogen-bond donor used in the ES formulation. For both tested cosolvents, the systems containing ethylene glycol-based ESs (BET:EG) or 1,3-propanediol-based ESs (BET:PROP) consistently

exhibited the largest biphasic regions. In contrast, systems containing urea (BET:U) and 1,4-butanediol (BET:BUT) showed smaller immiscibility regions. This behavior can be attributed to the polarity of the HBDs. When comparing the diols, ethylene glycol and 1,3-propanediol are more polar than 1,4-butanediol [85] (Table S9 in SM). This higher polarity likely increases the overall hydrophilicity of the resulting EG- and PROP-based ES, strengthening their affinity for the aqueous phase and thus increasing their immiscibility with the organic cosolvents over a wider compositional range. In the case of the BET:U system, despite its strong interaction with water [74], a direct comparison with the diol-based systems containing diols is restricted due to their structural differences. Conversely, the higher miscibility of the urea– and 1,4–butanediol–based ESs may pose a practical limitation for their recovery via liquid–liquid extraction.

When evaluating the effect of the cosolvent, 1-butanol generally resulted in a more extensive biphasic region than ethyl acetate in most cases. This suggests that the alcohol is a more effective phase-separating agent for these aqueous ES solutions, providing greater operational flexibility since the formation of two phases occurs over a wider compositional window.

It is noteworthy that most of the binodal curves do not include experimental points near the critical (plait) point. This is a limitation of the cloud point method, as the visual detection of the subtle turbidity in this region is inherently difficult, leading to a higher experimental [86–88]. However, for two systems, BET:PROP (Figure 5a) and BET:BUT (Figure 6a), compositions close to the plait point could be reliably determined. For the remaining systems, the phase separation was too indistinct in this region to be accurately measured.

Regarding the applied correlation approaches, the three-parameter Merchuk model [53] was chosen as it is a well-established approach for describing binodal curves of aqueous two-phase systems containing alternative solvents, while the five-parameter Hu model [54] was selected for comparison, as it has a higher number of adjustable parameters and was expected to provide a more precise correlation [77,89–92]. An analysis of statistical metrics (Tables 3 and 4) demonstrates the superior performance of the Hu model. The five-parameter model provided an excellent correlation for all systems, with coefficient of determination (R^2) values consistently greater than 0.995. In contrast, the three-parameter Merchuck model yielded less precise fits for the studied systems, with R^2 values ranging from 0.987 to 0.995. These differences are visually confirmed in Figures 3–6, where the Hu model accurately traces the entire composition ranges, whereas the Merchuk model exhibits higher deviations, particularly in the water-rich region.

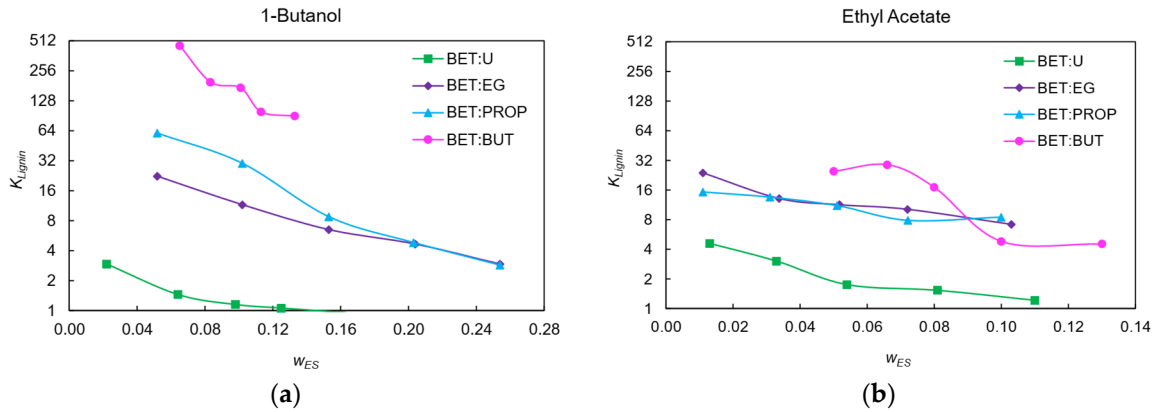
It is important to note that the Merchuk model was developed for aqueous systems with polyethylene glycol (PEG) and inorganic salts, which are chemically distinct from the ES and cosolvents evaluated in this work. Furthermore, the absence of experimental data near the critical region in most of the studied systems may have also contributed to the observed deviations, as such data were included in Merchuk's original work [53].

Given its evidenced robustness in describing the binodal curves, the Hu model was used to establish a qualitative ranking of the based on the extent of their biphasic regions of the aqueous systems. This ranking, from the largest to the smallest immiscibility area, is the following: BET:EG + 1-But ≈ BET:PROP + 1-But > BET:U + 1-But > BET:EG + EA ≈ BET:PROP + EA ≈ BET:BUT + 1-But > BET:BUT + EA > BET:U + EA.

3.2. Kraft Lignin Partitioning

The Kraft lignin partition coefficient (K_{Lignin}), defined in Equation (5), was measured to evaluate the distribution of lignin between the two phases. The results are summarized in Figure 7, which plots K_{Lignin} as a function of the global ES mass fraction for the systems containing 1-butanol (a) and ethyl acetate (b). The y-axis was plotted on a loga-

rithmic scale (base 2) to facilitate the visualization of the curves. For improved clarity, the curves presented in Figure 7 have been individually plotted in Figures S2–S5 (available in the SM). The complete experimental data, including the K_{Lignin} values, for the five distinct global mass compositions and the corresponding phase densities, are provided in Tables S10–S17 of the SM.



(**a**) (**b**)

Figure 7. Kraft lignin partition coefficient as a function of the ES global mass fraction for the systems containing 1-butanol (**a**) and ethyl acetate (**b**) as cosolvent.

The partitioning results (Figure 7, Tables S9–S16) show that the K_{Lignin} values were greater than 1 for nearly all the systems studied. The only exception was a single point in the {1-But + BET:U} system ($w_{BET:U}$ = 0.163), where K_{Lignin} was 0.9. This result indicates a strong preferential partitioning of lignin into the top, cosolvent-rich phase. This behavior is driven by the pronounced hydrophobic character of lignin [51], which has very low water solubility [19,42,51,93] and a higher affinity with organic-rich media [94]. Furthermore, while lignin is soluble in pure ESs, the literature confirms that its solubility drops sharply as the water content in the aqueous ES solution increases [19,42,93].

A second trend observed in Figure 7 is that K_{Lignin} values generally decrease as the overall mass fraction of ES increases. Due to their hydrophilic nature, the betaine-based solvents studied here are expected to concentrate in the bottom (aqueous) phase upon the addition of mildly polar organic cosolvent (e.g., ethyl acetate, 1-butanol), a behavior registered in the literature reports for other hydrophilic ESs [48,49]. Since ESs are typically good solvents for dissolving lignin [19,42,93,95], increasing their overall concentration in the system enhances the aqueous phase capacity to retain lignin, which in turn reduces the partition to the top phase.

The combination of these two behaviors—lignin preferentially migrating to the top phase while the ES tends to remain in the bottom phase [48,49,96]—indicates that liquid–liquid extraction using aqueous mixtures of 1-butanol or ethyl acetate could be a viable strategy for recovering Kraft lignin and enabling the potential for ESs reuse, which is in line with previous works [24,25,49].

Further analysis reveals that the lignin partition behavior is strongly dependent on the specific ES + cosolvent combination. For the systems based on the urea ES (BET:U), the partitioning was modest with both tested solvents: K_{Lignin} values ranged from 0.9 to 2.9 with 1-butanol and from 1.2 to 4.6 with ethyl acetate. Similarly, for the ethylene glycol ES (BET:EG), higher partition coefficients were obtained, but no substantial difference was observed between the systems containing 1-butanol ($2.9 \leq K_{Lignin} \leq 22.3$) and ethyl acetate ($7.2 \leq K_{Lignin} \leq 23.8$). In contrast, the choice of solvent had a much more pronounced impact on the systems containing 1,3-propanediol (BET:PROP) and 1,4-butanediol (BET:BUT). In the case of BET:PROP, a broader range of partition coefficient values was obtained when 1-butanol ($2.9 \leq K_{Lignin} \leq 60.4$) was used compared to ethyl acetate ($7.9 \leq K_{Lignin} \leq 15.3$).

For the systems with BET:BUT, very high partition coefficients were observed for the system with 1-butanol ($89.8 \leq K_{Lignin} \leq 456.5$), while ethyl acetate yielded significantly lower values, ranging from 4.5 to 24.7. These results demonstrate that the synergistic effect between the HBD and the cosolvent is the critical factor in achieving high lignin partition coefficients.

A comparison with previously reported data highlights the strong potential of the biphasic systems proposed in this work for the recovery of Kraft lignin from its mixtures with most of the investigated betaine-based solvents. For instance, Dias et al. (2020) [55] investigated the potential of water/acetone solutions to fractionate Kraft lignin/protic ionic liquids mixtures, reporting lignin partition coefficients in the range of 0.6 to 5.0. Similarly, Xin et al. (2012) [63] reported the partition coefficients of different lignin types in mixtures of ionic liquid ([C_2mim][OAc]) and water/ethyl acetate, water/1,4-dioxane and water/THF (tetrahydrofuran). For Kraft lignin, the ranges of partition coefficients were $0.0 \leq K_{Lignin} \leq 2.0$ for ethyl acetate, $0.0 \leq K_{Lignin} \leq 1.0$ for 1,4-dioxane, and $0.0 \leq K_{Lignin} \leq 4.0$ for tetrahydrofuran (THF). In the present study, higher partition coefficients were obtained for most of the tested systems, particularly for the BET:BUT + 1-butanol combination, which yielded partition coefficients that are orders of magnitude higher, evidencing a greater driving force for the transfer of lignin to the organic phase. The comparison is limited to IL-based systems due to the lack of reported data for eutectic solvents in the literature, which underscores the novelty of this work.

4. Conclusions

This work investigated the liquid–liquid equilibrium (LLE) and Kraft lignin partitioning in biphasic systems composed of betaine-based ES, water, and an organic cosolvent (butanol or ethyl acetate). For LLE modeling, the five-parameter Hu model generally provided a significantly more accurate description of the binodal curves than the Merchuk model. The experimental data showed that 1-butanol generally created larger biphasic regions compared to ethyl acetate, and in nearly all systems, lignin preferentially partitioned to the organic phase ($K_{Lignin} > 1$), supporting the viability of liquid–liquid extraction to separate lignin from the ES. A more detailed analysis revealed that 1-butanol also yielded substantially higher partition coefficients for the systems containing BET:PROP and BET:BUT, with the latter combination emerging as the most promising for lignin recovery. This system exhibited the highest lignin partition coefficient values, with values often exceeding 100 ($w_{BET:BUT} \leq 0.101$) and a maximum of 456.5 ($w_{BET:BUT} \leq 0.065$).

To the best of our knowledge, this is the first study to report liquid–liquid equilibrium data and Kraft lignin partition for systems containing betaine-based ESs. The results provide valuable insights for the design of lignin recovery processes and offer evidence that liquid–liquid extraction is a viable approach for the selective separation of lignin from these ESs, with 1-butanol emerging as a particularly effective cosolvent. This work contributes to expanding the limited experimental dataset for these systems, supporting the continued development of ESs-based processes for lignocellulosic biomass valorization strategies.

Supplementary Materials: The following supporting information can be downloaded at: https://www.mdpi.com/article/10.3390/pr13123784/s1, Figure S1: Calibration curve of the UV-Vis spectrophotometric analysis of Kraft lignin. The plot shows the Kraft lignin concentration in dimethyl sulfoxide (g/g) (y-axis) as a function of the absorbance at 280 nm (x-axis). The line represents the linear regression used to determine the lignin concentrations in the experiments; Figure S2: Kraft lignin partition coefficient as a function of the overall mass fraction of the BET:U eutectic solvent for systems containing (a) 1-butanol and (b) ethyl acetate; Figure S3: Kraft lignin partition coefficient as a function of the overall mass fraction of the BET:EG eutectic solvent for systems containing (a) 1-butanol and (b) ethyl acetate; Figure S4: Kraft lignin partition coefficient as a function of the

overall mass fraction of the BET:PROP eutectic solvent for systems containing (a) 1-butanol and (b) ethyl acetate; Figure S5: Kraft lignin partition coefficient as a function of the overall mass fraction of the BET:BUT eutectic solvent for systems containing (a) 1-butanol and (b) ethyl acetate; Table S1: Experimental mass fraction (w) data for the binodal curve of {1-butanol (1) + water (2) + BET:U (3)} at 298.15 K and 95.0 kPa; Table S2: Experimental mass fraction (w) data for the binodal curve of {ethyl acetate (1) + water (2) + BET:U (3)} at 298.15 K and 95.0 kPa; Table S3: Experimental mass fraction (w) data for the binodal curve of {1-butanol (1) + water (2) + BET:EG (3)} at 298.15 K and 95.0 kPa; Table S4: Experimental mass fraction (w) data for the binodal curve {ethyl acetate (1) + water (2) + BET:EG (3)} at 298.15 K and 95.0 kPa; Table S5: Experimental mass fraction (w) data for the binodal curve of {1-butanol (1) + water (2) + BET:PROP (3)} at 298.15 K and 95.0 kPa; Table S6: Experimental mass fraction (w) data for the binodal curve of {ethyl acetate (1) + water (2) + BET:PROP (3)} at 298.15 K and 95.0 kPa; Table S7: Experimental mass fraction (w) data for the binodal curve of {1-butanol (1) + water (2) + BET:BUT (3)} at 298.15 K and 95.0 kPa; Table S8: Experimental mass fraction (w) data for the binodal curve of {ethyl acetate (1) + water (2) + BET:BUT (3)} at 298.15 K and 95.0 kPa; Table S9: Et(30) parameters for alcohol HBDs studied in this work; Table S10: Global compositions (w), phase densities (d_{Top} and d_{Bottom}), and Kraft lignin partition coefficients (K_{Lignin}) for the {1-butanol (1) + water (2) + BET:U (3)} system; Table S11: Global compositions (w), phase densities (d_{Top} and d_{Bottom}), and Kraft lignin partition coefficients (K_{Lignin}) for the {ethyl acetate (1) + water (2) + BET:U (3)} system; Table S12: Global compositions (w), phase densities (d_{Top} and d_{Bottom}), and Kraft lignin partition coefficients (K_{Lignin}) for the {1-butanol (1) + water (2) + BET:EG (3)} system; Table S13: Global compositions (w), phase densities (d_{Top} and d_{Bottom}), and Kraft lignin partition coefficients (K_{Lignin}) for the {ethyl acetate (1) + water (2) + BET:EG (3)} system; Table S14: Global compositions (w), phase densities (d_{Top} and d_{Bottom}), and Kraft lignin partition coefficients (K_{Lignin}) for the {1-butanol (1) + water (2) + BET:PROP (3)} system; Table S15: Global compositions (w), phase densities (d_{Top} and d_{Bottom}), and Kraft lignin partition coefficients (K_{Lignin}) for the {ethyl acetate (1) + water (2) + BET:PROP (3)} system; Table S16: Global compositions (w), phase densities (d_{Top} and d_{Bottom}), and Kraft lignin partition coefficients (K_{Lignin}) for the {1-butanol (1) + water (2) + BET:BUT (3)} system; Table S17: Global compositions (w), phase densities (d_{Top} and d_{Bottom}), and Kraft lignin partition coefficients (K_{Lignin}) for the {ethyl acetate (1) + water (2) + BET:BUT (3)} system.

Author Contributions: F.S.A.: conceptualization, methodology, validation, investigation, data curation, formal analysis, writing (original draft), visualization, software. D.M.S.: validation, investigation, data curation. S.M.V.-B.: conceptualization, methodology, visualization, supervision, writing (review and editing). M.C.d.C.: conceptualization, resources, visualization, writing (review and editing), supervision, project administration, funding acquisition. All authors have read and agreed to the published version of the manuscript.

Funding: This study was financed, in part, by the Agência Nacional do Petróleo, Gás Natural e Biocombustíveis (ANP) through the Programa de Recursos Humanos (PRH—2024/10556-0). The authors are also grateful to The Coordination for the Improvement of Higher Education Personnel (CAPES, Brazil)—Finance Code 001, the National Council for Scientific and Technological Development (CNPq—312848/2023-4, 444231/2024-2, and 443214/2024-7), the São Paulo Research Foundation (FAPESP—2024/11984-6, 2024/01069-9, and 2025/20664-8) and FAEPEX Unicamp for the financial support.

Data Availability Statement: The original contributions presented in this study are included in the article/Supplementary Materials. Further inquiries can be directed to the corresponding authors.

Acknowledgments: The authors would also like to thank Suzano S.A. for providing the isolated Kraft lignin used in the assays.

Conflicts of Interest: The authors declare no conflicts of interest. The funding sponsors had no role in the design of the study; in the collection, analysis, or interpretation of data; in the writing of the manuscript; or in the decision to publish the results.

Abbreviations

The following abbreviations are used in this manuscript:

ES	Eutectic Solvent
LLE	Liquid–Liquid Equilibrium
DES	Deep Eutectic Solvent
HBA	Hydrogen-bond Acceptor
HBD	Hydrogen-bond Donor
BET	Betaine
U	Urea
EG	Ethylene Glycol
PROP	1,3-Propanediol
BUT	1,4-Butanediol
1-But	1-Butanol
EA	Ethyl Acetate
R^2	Coefficient of Determination
MSE	Mean Squared Error
DMSO	Dimethyl Sulfoxide
SM	Supplementary Materials
THF	Tetrahydrofuran

References

1. Rabaçal, M.; Ferreira, A.F.; Silva, C.A.M.; Costa, M. *Biorefineries: Targeting Energy, High Value Products and Waste Valorisation*; Lecture Notes in Energy; Springer: Cham, Switzerland, 2017; Volume 57.
2. Liu, X.; Wang, Y.; Duan, H. Recent Progress in Electrocatalytic Conversion of Lignin: From Monomers, Dimers, to Raw Lignin. *Precis. Chem.* **2024**, *2*, 428–446. [CrossRef]
3. Saral, J.S.; Satheesh, A.R.; Ranganathan, P. Economic and Environmental Analysis of Algal Biorefinery for the Production of Renewable Fuels and Co-Product. *Energy Convers. Manag. X* **2022**, *14*, 100189. [CrossRef]
4. Megía, P.J.; Vizcaíno, A.J.; Calles, J.A.; Carrero, A. Hydrogen Production Technologies: From Fossil Fuels toward Renewable Sources. A Mini Review. *Energy Fuels* **2021**, *35*, 16403–16415. [CrossRef]
5. Wagle, A.; Angove, M.J.; Mahara, A.; Wagle, A.; Mainali, B.; Martins, M.; Goldbeck, R.; Raj Paudel, S. Multi-Stage Pre-Treatment of Lignocellulosic Biomass for Multi-Product Biorefinery: A Review. *Sustain. Energy Technol. Assess.* **2022**, *49*, 101702. [CrossRef]
6. Agede, O.; Thies, M.C. Purification and Fractionation of Lignin via ALPHA: Liquid–Liquid Equilibrium for the Lignin–Acetic Acid–Water System. *ChemSusChem* **2024**, *17*, e202300989. [CrossRef] [PubMed]
7. Srivastava, N.; Singh, R.; Singh, P.; Ahmad, I.; Singh, R.P.; Rai, A.K.; Asiri, M.; Gupta, V.K. Recent Advances on Lignocellulosic Bioresources and Their Valorization in Biofuels Production: Challenges and Viability Assessment. *Environ. Technol. Innov.* **2023**, *29*, 103037. [CrossRef]
8. Cherubini, F. The Biorefinery Concept: Using Biomass Instead of Oil for Producing Energy and Chemicals. *Energy Convers. Manag.* **2010**, *51*, 1412–1421. [CrossRef]
9. Zhou, M.; Fakayode, O.A.; Ahmed Yagoub, A.E.; Ji, Q.; Zhou, C. Lignin Fractionation from Lignocellulosic Biomass Using Deep Eutectic Solvents and Its Valorization. *Renew. Sustain. Energy Rev.* **2022**, *156*, 111986. [CrossRef]
10. Kohli, K.; Prajapati, R.; Katuwal, S.; Kim, J.; Mullen, C.A.; Strahan, G.D.; Biswas, A.; Sharma, B.K. Maximization of Kraft Lignin Depolymerization Using Synthetic Mixed Oxide Catalysts under Microwave Exposure. *Ind. Crops Prod.* **2025**, *227*, 120787. [CrossRef]
11. Dias, R.M.; Da Costa Lopes, A.M.; Silvestre, A.J.D.; Coutinho, J.A.P.; Da Costa, M.C. Uncovering the Potentialities of Protic Ionic Liquids Based on Alkanolammonium and Carboxylate Ions and Their Aqueous Solutions as Non-Derivatizing Solvents of Kraft Lignin. *Ind. Crops Prod.* **2020**, *143*, 111866. [CrossRef]
12. Isikgor, F.H.; Becer, C.R. Lignocellulosic Biomass: A Sustainable Platform for the Production of Bio-Based Chemicals and Polymers. *Polym. Chem.* **2015**, *6*, 4497–4559. [CrossRef]
13. Manyatshe, A.; Sibali, L.L. A Review on the Recovery of Cellulose, Lignin, and Hemicellulose Biopolymers from the Same Source of Lignocellulosic Biomass—Methodology, Characterization and Applications. *J. Water Process Eng.* **2025**, *70*, 107037. [CrossRef]
14. Oriez, V.; Peydecastaing, J.; Pontalier, P.-Y. Lignocellulosic Biomass Mild Alkaline Fractionation and Resulting Extract Purification Processes: Conditions, Yields, and Purities. *Clean Technol.* **2020**, *2*, 91–115. [CrossRef]
15. Shorey, R.; Salaghi, A.; Fatehi, P.; Mekonnen, T.H. Valorization of Lignin for Advanced Material Applications: A Review. *RSC Sustain.* **2024**, *2*, 804–831. [CrossRef]

16. Umar, Y.; Velasco, O.; Abdelaziz, O.Y.; Aboelazayem, O.; Gadalla, M.A.; Hulteberg, C.P.; Saha, B. A Renewable Lignin-Derived Bio-Oil for Boosting the Oxidation Stability of Biodiesel. *Renew. Energy* **2022**, *182*, 867–878. [CrossRef]
17. García, M.; Botella, L.; Gil-Lalaguna, N.; Arauzo, J.; Gonzalo, A.; Sánchez, J.L. Antioxidants for Biodiesel: Additives Prepared from Extracted Fractions of Bio-Oil. *Fuel Process. Technol.* **2017**, *156*, 407–414. [CrossRef]
18. Pinho, A.D.R.; De Almeida, M.B.B.; Mendes, F.L.; Casavechia, L.C.; Talmadge, M.S.; Kinchin, C.M.; Chum, H.L. Fast Pyrolysis Oil from Pinewood Chips Co-Processing with Vacuum Gas Oil in an FCC Unit for Second Generation Fuel Production. *Fuel* **2017**, *188*, 462–473. [CrossRef]
19. Sosa, F.H.B.; Abranches, D.O.; Da Costa Lopes, A.M.; Da Costa, M.C.; Coutinho, J.A.P. Role of Deep Eutectic Solvent Precursors as Hydrotropes: Unveiling Synergism/Antagonism for Enhanced Kraft Lignin Dissolution. *ACS Sustain. Chem. Eng.* **2024**, *12*, 8930–8940. [CrossRef]
20. Brienza, F.; Cannella, D.; Montesdeoca, D.; Cybulska, I.; Debecker, D.P. A Guide to Lignin Valorization in Biorefineries: Traditional, Recent, and Forthcoming Approaches to Convert Raw Lignocellulose into Valuable Materials and Chemicals. *RSC Sustain.* **2024**, *2*, 37–90. [CrossRef]
21. Forssell, S.; Bangalore Ashok, R.P.; Henn, K.A.; Tirronen, E.; Toivonen, J.; Österberg, M.; Oinas, P. Techno-Economic Assessment of the Industrial-Scale Production of Epoxidized Kraft Lignin for Adhesives or Coatings. *ACS Sustain. Chem. Eng.* **2025**, *13*, 3200–3208. [CrossRef]
22. Gandla, M.L.; Martín, C.; Jönsson, L.J. Analytical Enzymatic Saccharification of Lignocellulosic Biomass for Conversion to Biofuels and Bio-Based Chemicals. *Energies* **2018**, *11*, 2936. [CrossRef]
23. Vu, H.P.; Nguyen, L.N.; Vu, M.T.; Johir, M.A.H.; McLaughlan, R.; Nghiem, L.D. A Comprehensive Review on the Framework to Valorise Lignocellulosic Biomass as Biorefinery Feedstocks. *Sci. Total Environ.* **2020**, *743*, 140630. [CrossRef]
24. Gholami, M.; Tijburg, J.M.; Schuur, B. Continuous Liquid–Liquid Extraction to Recover Lignin and Furanics from Lactic Acid: Choline Chloride Deep Eutectic Solvent after Cooking of Spruce. *Sep. Purif. Technol.* **2024**, *338*, 126526. [CrossRef]
25. Gholami, M.; Tijburg, J.M.; Schuur, B. Comparing Organic Solvents in a Combined Water Precipitation and Liquid–Liquid Extraction Process to Recover Lignin and Furanics from a Lactic Acid: Choline Chloride Deep Eutectic Solvent Used as Cooking Liquor for Cooking of Spruce. *Biomass Conv. Bioref.* **2024**, *14*, 25331–25342. [CrossRef]
26. Brännvall, E.; Norberg, L.; Karlström, K. Effect of Residual Alkali Level in Softwood Kraft Cooking. *Cellulose* **2024**, *31*, 9385–9394. [CrossRef]
27. Liu, X.; Bouxin, F.P.; Fan, J.; Budarin, V.L.; Hu, C.; Clark, J.H. Recent Advances in the Catalytic Depolymerization of Lignin towards Phenolic Chemicals: A Review. *ChemSusChem* **2020**, *13*, 4296–4317. [CrossRef]
28. Vilcocq, L.; Chaussard, N.; Hernández Mañas, A.; Boyron, O.; Taam, M.; Bertaud, F.; Fongarland, P.; Djakovitch, L. Potential of Catalytic Oxidation of Kraft Black Liquor for the Production of Biosourced Compounds. *Green Chem.* **2023**, *25*, 4793–4807. [CrossRef]
29. Argyropoulos, D.D.S.; Crestini, C.; Dahlstrand, C.; Furusjö, E.; Gioia, C.; Jedvert, K.; Henriksson, G.; Hulteberg, C.; Lawoko, M.; Pierrou, C.; et al. Kraft Lignin: A Valuable, Sustainable Resource, Opportunities and Challenges. *ChemSusChem* **2023**, *16*, e202300492. [CrossRef]
30. Crestini, C.; Lange, H.; Sette, M.; Argyropoulos, D.S. On the Structure of Softwood Kraft Lignin. *Green Chem.* **2017**, *19*, 4104–4121. [CrossRef]
31. Constant, S.; Wienk, H.L.J.; Frissen, A.E.; Peinder, P.D.; Boelens, R.; Van Es, D.S.; Grisel, R.J.H.; Weckhuysen, B.M.; Huijgen, W.J.J.; Gosselink, R.J.A.; et al. New Insights into the Structure and Composition of Technical Lignins: A Comparative Characterisation Study. *Green Chem.* **2016**, *18*, 2651–2665. [CrossRef]
32. Jiang, X.; Savithri, D.; Du, X.; Pawar, S.; Jameel, H.; Chang, H.; Zhou, X. Fractionation and Characterization of Kraft Lignin by Sequential Precipitation with Various Organic Solvents. *ACS Sustain. Chem. Eng.* **2017**, *5*, 835–842. [CrossRef]
33. Liu, R.; Smeds, A.; Wang, L.; Pranovich, A.; Hemming, J.; Willför, S.; Zhang, H.; Xu, C. Fractionation of Lignin with Decreased Heterogeneity: Based on a Detailed Characteristics Study of Sequentially Extracted Softwood Kraft Lignin. *ACS Sustain. Chem. Eng.* **2021**, *9*, 13862–13873. [CrossRef]
34. Cunha, S.C.; Fernandes, J.O. Extraction Techniques with Deep Eutectic Solvents. *TrAC Trends Anal. Chem.* **2018**, *105*, 225–239. [CrossRef]
35. Fakayode, O.A.; Wang, Z.; Wahia, H.; Mustapha, A.T.; Zhou, C.; Ma, H. Higher Heating Value, Exergy, Pyrolysis Kinetics and Thermodynamic Analysis of Ultrasound-Assisted Deep Eutectic Solvent Pretreated Watermelon Rind Biomass. *Bioresour. Technol.* **2021**, *332*, 125040. [CrossRef] [PubMed]
36. Ji, Q.; Yu, X.; Yagoub, A.E.-G.A.; Chen, L.; Fakayode, O.A.; Zhou, C. Synergism of Sweeping Frequency Ultrasound and Deep Eutectic Solvents Pretreatment for Fractionation of Sugarcane Bagasse and Enhancing Enzymatic Hydrolysis. *Ultrason. Sonochem.* **2021**, *73*, 105470. [CrossRef]

37. Ji, Q.; Yu, X.; Yagoub, A.E.A.; Chen, L.; Mustapha, A.T.; Zhou, C. Enhancement of Lignin Removal and Enzymolysis of Sugarcane Bagasse by Ultrasound-Assisted Ethanol Synergized Deep Eutectic Solvent Pretreatment. *Renew. Energy* **2021**, *172*, 304–316. [CrossRef]
38. Wang, H.; Meng, H.; Olowoyo, J.O.; Zeng, Y.; Zheng, Y. Advancements in Lignin Valorization for Energy Storage Applications: Sustainable Technologies for Lignin Extraction and Hydrothermal Carbonization. *Nanomaterials* **2025**, *15*, 309. [CrossRef]
39. Miao, G.; Li, H.; Zhu, Y.; Chen, S.; Lu, F.; Ralph, J.; Xu, F. Deep Eutectic Solvents for Efficient Fractionation of Lignocellulose to Produce Uncondensed Lignin and High-Quality Cellulose. *ACS Sustain. Chem. Eng.* **2025**, *13*, 2197–2209. [CrossRef]
40. Li, C.; Huang, C.; Zhao, Y.; Zheng, C.; Su, H.; Zhang, L.; Luo, W.; Zhao, H.; Wang, S.; Huang, L.-J. Effect of Choline-Based Deep Eutectic Solvent Pretreatment on the Structure of Cellulose and Lignin in Bagasse. *Processes* **2021**, *9*, 384. [CrossRef]
41. Chen, Z.; Ragauskas, A.; Wan, C. Lignin Extraction and Upgrading Using Deep Eutectic Solvents. *Ind. Crops Prod.* **2020**, *147*, 112241. [CrossRef]
42. Sosa, F.H.B.; Abranches, D.O.; Da Costa Lopes, A.M.; Coutinho, J.A.P.; Da Costa, M.C. Kraft Lignin Solubility and Its Chemical Modification in Deep Eutectic Solvents. *ACS Sustain. Chem. Eng.* **2020**, *8*, 18577–18589. [CrossRef]
43. Chen, H.; Wang, A.; Yan, C.; Liu, S.; Li, L.; Wu, Q.; Liu, Y.; Liu, Y.; Nie, G.; Nie, S.; et al. Study on the Solubility of Industrial Lignin in Choline Chloride-Based Deep Eutectic Solvents. *Sustainability* **2023**, *15*, 7118. [CrossRef]
44. Martins, M.A.R.; Pinho, S.P.; Coutinho, J.A.P. Insights into the Nature of Eutectic and Deep Eutectic Mixtures. *J Solut. Chem* **2019**, *48*, 962–982. [CrossRef]
45. Abranches, D.O.; Coutinho, J.A.P. Everything You Wanted to Know about Deep Eutectic Solvents but Were Afraid to Be Told. *Annu. Rev. Chem. Biomol. Eng.* **2023**, *14*, 141–163. [CrossRef] [PubMed]
46. Ferreira, C.; Sarraguça, M. A Comprehensive Review on Deep Eutectic Solvents and Its Use to Extract Bioactive Compounds of Pharmaceutical Interest. *Pharmaceuticals* **2024**, *17*, 124. [CrossRef] [PubMed]
47. Chen, Y.; Mu, T. Application of Deep Eutectic Solvents in Biomass Pretreatment and Conversion. *Green Energy Environ.* **2019**, *4*, 95–115. [CrossRef]
48. Smink, D.; Kersten, S.R.A.; Schuur, B. Recovery of Lignin from Deep Eutectic Solvents by Liquid-Liquid Extraction. *Sep. Purif. Technol.* **2020**, *235*, 116127. [CrossRef]
49. Smink, D.; Kersten, S.R.A.; Schuur, B. Comparing Multistage Liquid–Liquid Extraction with Cold Water Precipitation for Improvement of Lignin Recovery from Deep Eutectic Solvents. *Sep. Purif. Technol.* **2020**, *252*, 117395. [CrossRef]
50. Alvarez-Vasco, C.; Ma, R.; Quintero, M.; Guo, M.; Geleynse, S.; Ramasamy, K.K.; Wolcott, M.; Zhang, X. Unique Low-Molecular-Weight Lignin with High Purity Extracted from Wood by Deep Eutectic Solvents (DES): A Source of Lignin for Valorization. *Green Chem.* **2016**, *18*, 5133–5141. [CrossRef]
51. Dias, R.M.; Vilas-Boas, S.M.; Da Costa, M.C. Unveiling the Ability of Protic and Aprotic Ionic Liquids to Dissolve and Modify Kraft Lignin. *Sep. Purif. Technol.* **2024**, *350*, 127977. [CrossRef]
52. Kaul, A. The Phase Diagram. In *Aqueous Two-Phase Systems: Methods and Protocols*; Hatti-Kaul, R., Ed.; Methods in Biotechnology; Humana Press: Totowa, NJ, USA, 2000; Volume 11, pp. 11–21.
53. Merchuk, J.C.; Andrews, B.A.; Asenjo, J.A. Aqueous Two-Phase Systems for Protein Separation. *J. Chromatogr. B Biomed. Sci. Appl.* **1998**, *711*, 285–293. [CrossRef]
54. Hu, M.; Zhai, Q.; Liu, Z.; Xia, S. Liquid−Liquid and Solid−Liquid Equilibrium of the Ternary System Ethanol + Cesium Sulfate + Water at (10, 30, and 50) °C. *J. Chem. Eng. Data* **2003**, *48*, 1561–1564. [CrossRef]
55. Dias, R.M.; Netto, G.C.A.; Petrin, L.C.G.; Pelaquim, F.P.; Sosa, F.H.B.; Costa, M.C.D. Aqueous Two-Phase System Formed by Alkanolammonium-Based Protic Ionic Liquids and Acetone: Experimental Data, Thermodynamic Modeling, and Kraft Lignin Partition. *Sep. Purif. Technol.* **2020**, *250*, 117207. [CrossRef]
56. Abranches, D.O.; Silva, L.P.; Martins, M.A.R.; Pinho, S.P.; Coutinho, J.A.P. Understanding the Formation of Deep Eutectic Solvents: Betaine as a Universal Hydrogen Bond Acceptor. *ChemSusChem* **2020**, *13*, 4916–4921. [CrossRef] [PubMed]
57. Fanali, C.; Della Posta, S.; Dugo, L.; Gentili, A.; Mondello, L.; De Gara, L. Choline-Chloride and Betaine-Based Deep Eutectic Solvents for Green Extraction of Nutraceutical Compounds from Spent Coffee Ground. *J. Pharm. Biomed. Anal.* **2020**, *189*, 113421. [CrossRef]
58. Liu, Y.; Friesen, J.B.; McAlpine, J.B.; Lankin, D.C.; Chen, S.-N.; Pauli, G.F. Natural Deep Eutectic Solvents: Properties, Applications, and Perspectives. *J. Nat. Prod.* **2018**, *81*, 679–690. [CrossRef]
59. Mustafa, S.M.; Barzinjy, A.A.; Hamad, A.H.; Hamad, S.M. Betaine-Based Deep Eutectic Solvents Mediated Synthesis of Zinc Oxide Nanoparticles at Low Temperature. *Ceram. Int.* **2022**, *48*, 28951–28960. [CrossRef]
60. Han, Y.; Paiva Pinheiro Pires, A.; Denson, M.; McDonald, A.G.; Garcia-Perez, M. Ternary Phase Diagram of Water/Bio-Oil/Organic Solvent for Bio-Oil Fractionation. *Energy Fuels* **2020**, *34*, 16250–16264. [CrossRef]
61. Isci, A.; Kaltschmitt, M. Recovery and Recycling of Deep Eutectic Solvents in Biomass Conversions: A Review. *Biomass Conv. Bioref.* **2022**, *12*, 197–226. [CrossRef]

62. Pan, J.; Fu, J.; Deng, S.; Lu, X. Distribution Coefficient of Products from Lignin Oxidative Degradation in Organic-Water Systems. *Fuel Process. Technol.* **2015**, *140*, 262–266. [CrossRef]
63. Xin, Q.; Pfeiffer, K.; Prausnitz, J.M.; Clark, D.S.; Blanch, H.W. Extraction of Lignins from Aqueous–Ionic Liquid Mixtures by Organic Solvents. *Biotechnol. Bioeng.* **2012**, *109*, 346–352. [CrossRef] [PubMed]
64. Rodrigues, L.A.; Cardeira, M.; Leonardo, I.C.; Gaspar, F.B.; Radojčić Redovniković, I.; Duarte, A.R.C.; Paiva, A.; Matias, A.A. Deep Eutectic Systems from Betaine and Polyols—Physicochemical and Toxicological Properties. *J. Mol. Liq.* **2021**, *335*, 116201. [CrossRef]
65. Zeng, C.-X.; Qi, S.-J.; Xin, R.-P.; Yang, B.; Wang, Y.-H. Synergistic Behavior of Betaine–Urea Mixture: Formation of Deep Eutectic Solvent. *J. Mol. Liq.* **2016**, *219*, 74–78. [CrossRef]
66. Fu, X.; Qiao, J.; Xu, Z.; Xu, C.; Li, X. Deep Eutectic Solvent Cocktail Enhanced the Pretreatment Efficiency of Lignocellulose. *Ind. Crops Prod.* **2024**, *210*, 118040. [CrossRef]
67. Fan, Y.; Ji, H.; Ji, X.; Tian, Z.; Chen, J. A Deep Eutectic Solvent with a Lignin Stabilization and Functionalization for Lignocellulosic Biomass Pretreatment. *Chem. Eng. J.* **2024**, *499*, 156482. [CrossRef]
68. Li, N.; Wang, Y.; Xu, K.; Huang, Y.; Wen, Q.; Ding, X. Development of Green Betaine-Based Deep Eutectic Solvent Aqueous Two-Phase System for the Extraction of Protein. *Talanta* **2016**, *152*, 23–32. [CrossRef]
69. Ribeiro, B.D.; De Carvalho Iff, L.; Coelho, M.A.Z.; Marrucho, I.M. Influence of Betaine- and Choline-Based Eutectic Solvents on Lipase Activity. *CBE* **2019**, *5*, 57–68. [CrossRef]
70. Kučan, K.Z.; Perković, M.; Cmrk, K.; Načinović, D.; Rogošić, M. Betaine + (Glycerol or Ethylene Glycol or Propylene Glycol) Deep Eutectic Solvents for Extractive Purification of Gasoline. *ChemistrySelect* **2018**, *3*, 12582–12590. [CrossRef]
71. Mulia, K.; Krisanti, E.; Nasruddin; Libriandy, E. Betaine-Based Deep Eutectic Solvents with Diol, Acid and Amine Hydrogen Bond Donors for Carbon Dioxide Absorption. *J. Phys. Conf. Ser.* **2019**, *1295*, 012039. [CrossRef]
72. Nowacki, K.; Wysokowski, M.; Galiński, M. Synthesis and Characterization of Betaine-Based Natural Deep Eutectic Solvents for Electrochemical Application. *J. Mol. Liq.* **2025**, *424*, 127071. [CrossRef]
73. Abbott, A.P.; Capper, G.; Davies, D.L.; Rasheed, R.K.; Tambyrajah, V. Novel Solvent Properties of Choline Chloride/Urea mixtures. *Chem. Commun.* **2003**, 70–71. [CrossRef]
74. Abranches, D.O.; Silva, L.P.; Martins, M.A.R.; Coutinho, J.A.P. Differences on the Impact of Water on the Deep Eutectic Solvents Betaine/Urea and Choline/Urea. *J. Chem. Phys.* **2021**, *155*, 034501. [CrossRef]
75. Eisa, M.; Ragauskaitė, D.; Shi, J.; Shimizu, S.; Bucko, T.; Williams, C.; Baltrusaitis, J. Interactions of Urea Surfaces with Water as Relative Humidity Obtained from Dynamic Vapor Sorption Experiments, In Situ Single-Particle Raman Spectroscopy, and Ab Initio Calculations. *ACS Earth Space Chem.* **2023**, *7*, 2139–2153. [CrossRef]
76. Werner, E.A. Urea as a Hygroscopic Substance. *Nature* **1937**, *139*, 512. [CrossRef]
77. Mashhaditafreshi, S.; Haghtalab, A. Study on Drug Separation in Two-Phase Aqueous Systems Using Deep Eutectic Solvent Consisting of Choline Chloride and 1,2 Propanediol. *J. Mol. Liq.* **2024**, *393*, 123603. [CrossRef]
78. Li, M.; Zhu, C.; Fu, T.; Gao, X.; Ma, Y. Effect of Water on Amine-Based Deep Eutectic Solvents (Choline Chloride + Monoethanolamine): Structure and Physicochemical Properties. *J. Environ. Chem. Eng.* **2022**, *10*, 106952. [CrossRef]
79. Karimi, S.; Shekaari, H. Application of Acidic Deep Eutectic Solvents in Green Extraction of 5-Hydroxymethylfurfural. *Sci. Rep.* **2022**, *12*, 13113. [CrossRef] [PubMed]
80. Vessally, E.; Rzayev, R. Application of Deep Eutectic Solvent-Based Aqueous Two Phase Systems for Extraction of Analgesic Drugs. *RSC Adv.* **2024**, *14*, 34253–34260. [CrossRef]
81. Hatfield, R.; Fukushima, R.S. Can Lignin Be Accurately Measured? *Crop Sci.* **2005**, *45*, 832–839. [CrossRef]
82. Kline, L.M.; Hayes, D.G.; Womac, A.R.; Labbé, N. Simplified Determination of Lignin Content in Hard and Soft Woods via UV-Spectrophotometric Analysis of Biomass Dissolved in Ionic Liquids. *BioRes* **2010**, *5*, 1366–1383. [CrossRef]
83. Sun, R.; Tomkinson, J.; Mao, F.C.; Sun, X.F. Physicochemical Characterization of Lignins from Rice Straw by Hydrogen Peroxide Treatment. *J. Appl. Polym. Sci.* **2001**, *79*, 719–732. [CrossRef]
84. Moré, J.J. The Levenberg-Marquardt Algorithm: Implementation and Theory. In *Numerical Analysis*; Watson, G.A., Ed.; Lecture Notes in Mathematics; Springer: Berlin/Heidelberg, Germany, 1978; Volume 630, pp. 105–116.
85. Saini, V.; Singh, H. Predicting the ET(30) Parameter of Organic Solvents via Machine Learning. *Chem. Phys. Lett.* **2023**, *826*, 140672. [CrossRef]
86. Kazakov, S.V.; Chernova, N.I. Properties of the Liquid-Liquid Coexistence Curves with Several Critical Points. *Chem. Eng. Commun.* **2003**, *190*, 213–235. [CrossRef]
87. Losada-Pérez, P.; Pérez-Sánchez, G.; Cerdeiriña, C.A.; Troncoso, J.; Romaní, L. Thermodynamic Consistency near the Liquid-Liquid Critical Point. *J. Chem. Phys.* **2009**, *130*, 044506. [CrossRef]
88. Toikka, A.; Toikka, M. Solubility and Critical Phenomena in Reactive Liquid–Liquid Systems. *Pure Appl. Chem.* **2009**, *81*, 1591–1602. [CrossRef]

89. Barroca, L.R.; Velho, P.; Macedo, E.A. Novel Green Aqueous Two-Phase Systems (ATPSs) Based on Choline Salts and Application to the Removal of Pharmaceutical Pollutants from Water. *Fluid Phase Equilibria* **2024**, *586*, 114193. [CrossRef]
90. Sosa, F.H.B.; Farias, F.O.; Igarashi-Mafra, L.; Mafra, M.R. Measurement and Correlation of Aqueous Two-Phase Systems of Polyvinylpyrrolidone (PVP) and Manganese Sulfate: Effects of Molecular Weight and Temperature. *Fluid Phase Equilibria* **2018**, *472*, 204–211. [CrossRef]
91. Zafarani-Moattar, M.T.; Shekaari, H.; Pourbagherian, E. Study of the Liquid-Liquid Equilibrium for Aqueous Ternary Systems Containing Choline Bitartrate and 1-Propanol or 2-Propanol at Different Temperatures and Their Performances in Acetaminophen Separation and Alcohols Recovery. *Fluid Phase Equilibria* **2020**, *514*, 112536. [CrossRef]
92. Souza, I.N.; Rodrigues, L.C.V.; Soares, C.M.F.; Buarque, F.S.; Souza, R.L.; Lima, Á.S. Deep Eutectic Solvent-Based Aqueous Two-Phase Systems and Their Application in Partitioning of Phenol Compounds. *Molecules* **2024**, *29*, 4383. [CrossRef]
93. Soares, B.; Tavares, D.J.P.; Amaral, J.L.; Silvestre, A.J.D.; Freire, C.S.R.; Coutinho, J.A.P. Enhanced Solubility of Lignin Monomeric Model Compounds and Technical Lignins in Aqueous Solutions of Deep Eutectic Solvents. *ACS Sustain. Chem. Eng.* **2017**, *5*, 4056–4065. [CrossRef]
94. Dastpak, A.; Lourençon, T.V.; Balakshin, M.; Farhan Hashmi, S.; Lundström, M.; Wilson, B.P. Solubility Study of Lignin in Industrial Organic Solvents and Investigation of Electrochemical Properties of Spray-Coated Solutions. *Ind. Crops Prod.* **2020**, *148*, 112310. [CrossRef]
95. Zhang, Y.; Ren, H.; Li, B.; Udin, S.M.; Maarof, H.; Zhou, W.; Cheng, F.; Yang, J.; Liu, Y.; Alias, H.; et al. Mechanistic Insights into the Lignin Dissolution Behavior in Amino Acid Based Deep Eutectic Solvents. *Int. J. Biol. Macromol.* **2023**, *242*, 124829. [CrossRef]
96. Gomes, I.P.; Dos Santos, N.P.; Noronha, P.B.; Duarte, R.R.B.; Cardim, H.P.; Da Silva, E.A.; Dos Santos, R.J.; Ferreira-Pinto, L.; Arce, P. Multiphase Behavior of the Water + 1-Butanol + Deep Eutectic Solvent Systems at 101.3 kPa. *Molecules* **2024**, *29*, 4814. [CrossRef]

Disclaimer/Publisher's Note: The statements, opinions and data contained in all publications are solely those of the individual author(s) and contributor(s) and not of MDPI and/or the editor(s). MDPI and/or the editor(s) disclaim responsibility for any injury to people or property resulting from any ideas, methods, instructions or products referred to in the content.